J Mater Sci (2006) 41:7691–7695
DOI 10.1007/s10853-006-0608-4

Grain boundary order-disorder transitions

Ming Tang · W. Craig Carter · Rowland M. Cannon

Received: 29 April 2006 / Accepted: 20 June 2006 / Published online: 31 October 2006

Abstract The conditions for grain boundary (GB) structural transitions are determined from a diffuse interface model that incorporates structural disorder and crystallographic orientation. A graphical construction and numerical calculations illustrate the existence of a first-order GB order–disorder transition below the bulk melting point. When thermodynamic conditions permit their existence, disordered GB structures tend to be stable at higher temperatures and are perfectly wet by liquid at the melting point, while ordered grain boundaries are meta-stable against preferential melting. We calculate GB phase diagrams which are analogous to those for liquid–vapor phase transitions.

The possibility that a grain boundary (GB) may start to melt below the bulk melting point has long been speculated. The existence of its free surface counterpart, surface melting, has been confirmed by experiments [1–3]. Indirect evidence of GB premelting has been accumulated over decades from observations of abrupt changes in macroscopic properties such as GB diffusivities, dihedral angles, sliding and migration rates [4–8]. However, only limited direct evidence of GB premelting has been published. Hsieh and Baluffi imaged boundaries in pure aluminum by TEM [9]. They concluded that GB preferential melting does not occur below $0.999T_{\mathrm{m}}$. Recent direct observations confirm GB premelting in colloidal crystals [10] and in multi-component metallic systems [11].

Numerous atomistic calculations and simulations have been performed to study GB premelting, including lattice-gas models [12, 13], molecular dynamics (MD) [14–21], and Monte Carlo (MC) simulations [22, 23]. Although atomistic methods provide direct and often accurate calculations of GB structures and energies, such calculations are not feasible to predict GB behavior over a range of temperature, stress, chemical potentials, misorientations, and inclinations. Using a diffuse interface model developed by Kobayashi, Warren and Carter (KWC) [24, 25], we present an analysis of GB structures in the framework of classical interfacial thermodynamics. The analysis produces predictions of stability of different GB structures from general characteristics of thermodynamic data.

For material systems with fixed stoichiometry, the KWC model uses two coarse-grained field variables to describe a two-dimensional polycrystalline structure: a local crystallographic orientation field, $\theta(\vec{x})$, and a local crystallinity field, $\eta(\vec{x})$, which characterizes structure disorder. Readers are referred to the appendix in Ref. [26] for discussion on coarse-graining schemes to calculate η and θ.

For a GB plane in which both fields are uniform, η and θ reduce to functions of a single spatial variable x. Although the GB is diffuse in this model, its position can be identifies as a narrow region where η is significantly less than 1; θ changes abruptly at the minimum of $\eta(x)$ as illustrated in Fig. 1.

M. Tang (✉) · W. C. Carter
Department of Materials Science and Engineering, Massachusetts Institute of Technology, Cambridge, MA 02139, USA
e-mail: mingtang@mit.edu

R. M. Cannon
Lawrence Berkeley National Laboratory, Berkeley, CA 94720, USA

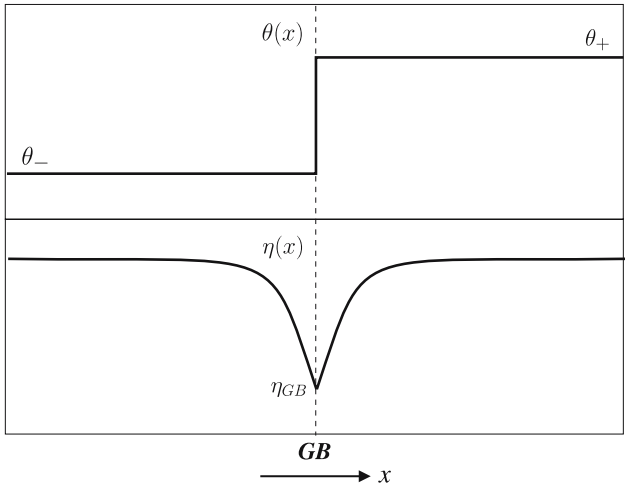

Fig. 1 Illustration of the profiles of the local crystallinity η and local orientation θ across a planar GB

The GB excess free energy is modeled as following:

$$F[\eta,\theta;T]=\int_{\mathcal{L}^{sys}}\left\{\Delta f(\eta(x);T)+\frac{v^2}{2}\left(\frac{d\eta}{dx}\right)^2+sg(\eta(x))\left|\frac{d\theta}{dx}\right|\right\}dx \quad (1)$$

where Δf is the excess homogeneous free energy density with respect to the single crystal reference state, i.e., $\Delta f(\eta = 1;\ T) = 0$. Δf is independent of θ because the homogeneous free energy density must be invariant under rotation of reference frame. At temperatures close to the melting point T_m, both crystalline and liquid state are local energy minima and thus $\Delta f(\eta;T)$ should have a double well form. The following expression has been used for Δf in previous papers [25, 26],

$$\Delta f(\eta;T)=\frac{\Delta H_m\Delta T}{T_m}\phi(\eta)+\frac{a^2}{2}\eta^q(1-\eta)^q \quad (2)$$

where $q \geq 2$ and

$$\phi(\eta)=(1-\eta)^3(1+3\eta+6\eta^2) \quad (3)$$

$\phi(\eta)$ is a sigmoidal interpolation between $\phi(0) = 1$ and $\phi(1) = 0$. The second term on the right hand side of Eq. 2 represents an energy barrier between crystalline and liquid states, where a^2 prescribes the barrier height. v and s in Eq. 1 are coefficients of the crystallinity and orientation gradient terms. The prefactor function $g(\eta)$ arises from the coupling between structural disorder and orientation gradient penalty: the penalty should decrease with increasing structural disorder and it vanishes in the liquid state. $g(\eta)$ can be a power function, i.e., $g(\eta) = \eta^p$, to reflect the coupling, but, on physical grounds, the exponent $p > 1$ [26].

The profiles of $\eta(x)$ and $\theta(x)$ of an equilibrium GB can be solved from the Euler equations that produce minimum of Eq. 1. It is shown [27] that if assuming $\eta(x)$ has a single local minimum at the GB core, the equilibrium $\theta(x)$ solution should be a step function that concentrates all its change at the GB center (assumed to be at $x = 0$), i.e.,

$$\theta^{eq}(x)=\theta_-+\Delta\theta H(x) \quad (4)$$

where $H(x)$ is a unit step function and $\Delta\theta \equiv \theta_+ - \theta_-$. Assuming $\eta(x)$ is symmetrical about the GB and applying Eq. 4 to Eq. 1, the GB excess energy reduces to a functional of $\eta(x)$

$$F[\eta(x);\Delta\theta,T]=s\Delta\theta g(\eta_{GB})+2\int_0^\infty\left[\Delta f(\eta;T)+\frac{v^2}{2}\left(\frac{d\eta}{dx}\right)^2\right]dx \quad (5)$$

where $\eta_{GB} = \eta(x = 0)$ is the local crystallinity at GB center and $\Delta\theta > 0$ is assumed.

The Euler equation for $F[\eta(x);\Delta\theta,T]$ is

$$v^2\frac{d^2\eta}{dx^2}=\frac{\partial\Delta f}{\partial\eta} \quad (6)$$

with the boundary conditions

$$\left.\frac{d\eta}{dx}\right|_{x=0^+}=\left.\frac{s\Delta\theta}{2v^2}\frac{dg}{d\eta}\right|_{\eta=\eta_{GB}} \quad (7)$$

$$\eta|_{x=+\infty}=1 \quad (8)$$

The first integral of Eq. 6 is

$$\frac{v^2}{2}\left(\frac{d\eta}{dx}\right)^2=\Delta f(\eta;T) \quad (9)$$

Inserting Eq. 9 into Eqs. 5 and 7 and changing the integration variable from x to η, we obtain another form of GB excess free energy and an equation that determines the equilibrium value of $\eta^{eq}{}_{GB}$:

$$\frac{F}{2}=\int_0^{\eta_{GB}}\frac{s\Delta\theta}{2}\frac{dg}{d\eta}(\eta)d\eta+\int_{\eta_{GB}}^1\sqrt{2v^2\Delta f(\eta;T)}d\eta \quad (10)$$

$$\sqrt{2v^2\Delta f(\eta_{GB};T)}=\left.\frac{s\Delta\theta}{2}\frac{dg}{d\eta}\right|_{\eta=\eta_{GB}} \quad (11)$$

Solutions to Eqs. 10 and 11 can be represented graphically, as illustrated in Fig. 2(a). By plotting $\sqrt{2v^2\Delta f}$ and $(s\Delta\theta/2)$ dg/dη as functions of η, $\eta^{eq}{}_{GB}$ is determined by the intersection(s) of the two curves. One half of the GB energy, $F/2$, is the area under the first curve between 0 and $\eta^{eq}{}_{GB}$ plus the area under the second curve between $\eta^{eq}{}_{GB}$ and 1. This graphic construction is similar to the approach used by Cahn in his critical point wetting theory; in fact, the functional Eq. 10 is isomorphic to Eq. 4 in Cahn's original description of critical point wetting [28]. The possibility of a first-order GB order–disorder transition below T_m is illustrated in Fig. 2(b). At temperatures significantly below T_m, e.g., T_1 in Fig. 2(b), the two curves intersect once at an $\eta^{eq}{}_{GB}$ close to 1, which predicts a relatively ordered GB structure. When increasing T toward T_m, the meta-stable minimum of Δf at $\eta = 0$ is lowered gradually to 0, causing the two curves to approach each other at low $\eta^{eq}{}_{GB}$. At T_2 ($> T_1$) in Fig. 2(b), three intersections are produced. The rightmost intersection represents an ordered GB that also exists at T_1. The leftmost intersection represents a (meta-)stable disordered GB of crystallinity η_{GB}^{eq-dis},while the middle one is an unstable solution because it maximizes the area below the two curves. According to the graphic construction of GB excess energy, the relative stability of the two solutions for ordered and disordered GBs depends on the difference between area A and B shown in Fig. 2(b). When the three-intersection configuration first appears with increasing T, area A is less than B and the ordered GB solution is more stable. Because area A increases with temperature, it may become larger than B at higher T; if so, the disordered GB becomes the more stable structure. At the temperature where area A equals B, a first-order GB transition occurs and the equilibrium GB crystallinity and thickness have a discontinuity. Fig. 2 also shows that the intersection for the ordered GB may merge with the middle intersection and disappear at temperatures very close to T_m, leaving the disordered GB as the only stable structure. As $T \to T_m$, it has been shown [26] that $\eta_{GB}^{eq-dis} \to 0$ and the thickness of the disordered GB diverges logarithmically. Therefore, the disordered GB is perfectly wet by liquid (i.e., its stable thickness is unbounded) at the melting point.

The existence of a first-order GB transition can also be seen from the $\Delta\theta - \eta_{GB}$ diagram. $\Delta\theta$ can be expressed as a function of η_{GB} and T with Eq. 11 as

$$\Delta\theta = \frac{2\sqrt{2v^2\Delta f(\eta_{GB};T)}}{s\dfrac{dg}{d\eta}(\eta_{GB})} \tag{12}$$

$\Delta\theta$ vs. η_{GB} is plotted at different fixed values of T (isotherms) in Fig. 3 with model parameters $g(\eta) = \eta^2$ and $q = 4$ in Eq. 2. $\Delta\theta$ and T in the plot are non-dimensionalized as $\tilde{\Delta\theta} = s\Delta\theta/(av)$ and $\tilde{T} = \Delta H_m (T - T_m)/(a^2 T_m)$ (the tilde signs above the rescaled variables are dropped in the figure for convenience). Figure 3 shows that at relatively low temperatures (curves with colors from green to red (pdf version)), GBs have increased disorder with increased misorientation. However, a local minimum and maximum appear on the curve above a critical temperature. Misorientations with values between the local minimum and maximum have three corresponding $\eta^{eq}{}_{GB}$ values: the middle one is an unstable solution, and the other two are solutions for a (meta-)stable ordered or disordered GB. Among these misorientations, there exists one $\Delta\theta$ that has two GB solutions with equal energies. This particular misorientation is indicated by a horizontal tie line (dashed black) in Fig.3. A tie-line divides a $\Delta\theta - \eta_{GB}$ curve into three parts, i.e., the disordered GB fraction above the line, the ordered GB

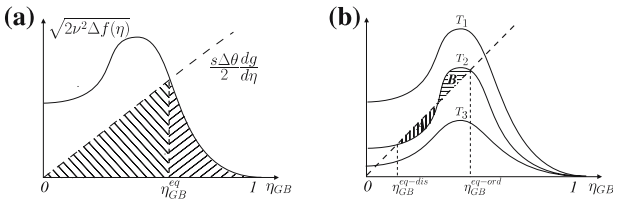

Fig. 2 (**a**) Graphical determination of the equilibrium GB crystallinity $\eta^{eq}{}_{GB}$ and excess energy F. $\eta^{eq}{}_{GB}$ is the intersection of the two curves in the figure, and $F/2$ is equal to the hatched area. (**b**) Illustration of a possible GB order–disorder transition below the melting point. $T_1 < T_2 < T_3 < T_m$. At $T = T_2$, two (meta-)stable GB structure exist, whose local crystallinities are η_{GB}^{eq-ord} (ordered GB) and η_{GB}^{eq-dis} (disordered GB)

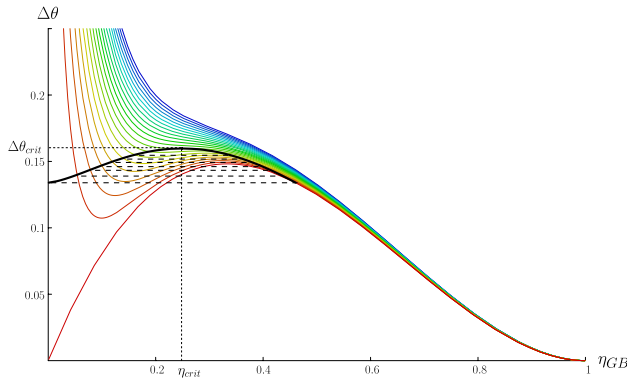

Fig. 3 Isotherms of $\Delta\theta - \eta_{GB}$ from Eq. 12 and Eq. 2. The temperature and misorientation values in the plot are rescaled as $\Delta H_m (T-T_m)/(a^2 T_m)$ and $s\Delta\theta/(av)$, respectively. The temperatures of the curves range from -5×10^{-4} (blue) to 0 (red). The critical point of the GB transition is numerically determined to be $T_{crit} = -2.00 \times 10^{-4}$, $\Delta\theta_{crit} = 0.160$, and $\eta_{crit} = 0.249$

fraction below the line, and the fraction between the two end-points of the tie-line that describes meta-stable GB states. The end-points of all the tie-lines at each temperature form two curves that bound the region of stability (solid black) for the ordered and disordered GBs. The two lines meet at a critical point, ($T_{\rm crit}$, $\Delta\theta_{\rm crit}$, $\eta_{\rm crit}$), which satisfies the following conditions

$$\begin{aligned} 0 &= \left.\frac{\partial \Delta\theta}{\partial \eta_{\rm GB}}\right|_{\eta_{GB}=\eta_{\rm crit},T=T_{\rm crit}} \\ 0 &= \left.\frac{\partial^2 \Delta\theta}{\partial \eta_{\rm GB}^2}\right|_{\eta_{GB}=\eta_{\rm crit},T=T_{\rm crit}} \\ \Delta\theta_{\rm crit} &= \frac{2\sqrt{2v^2\Delta f(\eta_{\rm crit};T_{\rm crit})}}{s\dfrac{{\rm d}g}{{\rm d}\eta}(\eta_{\rm crit})} \end{aligned} \tag{13}$$

The $\Delta\theta$–$\eta_{\rm GB}$ behavior in Fig. 3 is similar to the isotherms in a P–V diagram when there is a liquid–vapor phase transition. The boundary lines for ordered and disordered GBs are analogous to the saturated vapor and liquid lines. In Fig. 4, $\Delta\theta$ is plotted against T at constant η_{GB}, and the result is analogous to the P–T diagram of liquid-vapor transitions. Two families of constant crystallinity curves can be identified in Fig. 4. One family of curves (with colors from blue to yellow) have non-zero $\Delta\theta$ values at the melting point, while in the other family (colors from orange to red) $\Delta\theta$ diminishes to zero when approaching $T_{\rm m}$. The two groups of curves represent ordered and disordered GB structures, respectively. The boundary of the region where curves from both families cross is shown as two dashed lines in Fig. 4. It signifies the spinodals (or stability limits) of the two GB structures—the upper boundary is the spinodal line of ordered GBs and the lower boundary is for disordered GBs. The boundary lines for ordered and disordered GBs in Fig. 3 become a single coexistence line (solid black), $\Delta\theta_{CE}(T)$, in Fig. 4. This line and the two spinodal lines end at the critical point that is determined by Eq. 13. According to Fig. 4, grain boundaries can be categorized into three groups:

$\Delta\theta > \Delta\theta_{\rm crit}$, GBs disorder continuously and are completely melted at $T_{\rm m}$;
$\Delta\theta_{CE}(T_{\rm m}) < \Delta\theta < \Delta\theta_{\rm crit}$,GBs undergo a first-order premelting transition that also leads to perfect wetting at $T_{\rm m}$;
$\Delta\theta < \Delta\theta_{CE}(T_{\rm m})$, no transition occurs and GB structures remain ordered up to $T_{\rm m}$.

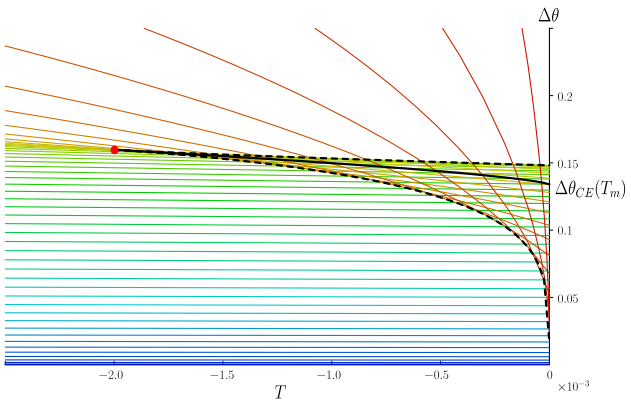

Fig. 4 $\Delta\theta$ – T plot under constant $\eta_{\rm GB}$ for the material parameters as those for Fig. 3. Colors of the curves indicate η_{GB} values ranging from 1 (blue) to 0 (red). Three characteristics lines are shown in the figure. Two dashed black lines are spinodals of ordered (upper) and disordered (lower) GBs, and the solid black line is a first-order transition line on which ordered and disordered GBs coexist. All three lines terminate at a critical point which is also shown in Fig. 3

The GB structural transitions illustrated by Fig. 2–4 may not appear in all material systems. Their existence depends on the shapes of functions Δf and $g(\eta)$ [26]. For example, if choosing $q = 2$ in Eq. 2 instead of $q = 4$, the energy barrier between the liquid and crystalline states becomes less deep and it is shown [26] that the coexistence curve shrinks to a single point $\Delta\theta = av/s$ at $T_{\rm m}$. GBs either melt continuously with $\Delta\theta < av/s$ or remain partially ordered at $T_{\rm m}$ with $\Delta\theta < av/s$, and there is no GB transition producing discontinuous structural attributes.

We have shown by graphical construction and numerical examples that grain boundaries may undergo an order–disorder transition at temperatures below the melting point. This transition is analogous to the liquid-vapor transition, as both are first-order and have a critical point on the coexistence curve. At the melting point, disordered GBs completely melt and are perfectly wet by liquid, but ordered GBs remain meta-stable against wetting. Finally, a similar but more complicated analysis can be applied to systems where local concentration is allowed to vary. A coupled premelting/prewetting transition is predicted to occur below the eutectic point and below the solidus line in binary eutectic systems. Details of this work are published elsewhere [29].

Acknowledgements Discussions with Yet-Ming Chiang and Jian Luo are gratefully acknowledged.

References

1. Frenken JWM, van der Veen JF (1985). Phys Rev Lett 54:134
2. Frenken JWM, Maree PMJ, van der Veen JF (1986) Phys Rev B 34:7506
3. Dash JG (1989) Cont Phys 30:89

4. Gleiter H (1970) Z Metallkd 61:282
5. Demianczuk DW, Aust KT (1975) Acta Metall 23:1149
6. Watanabe T, Kimura SI, Karashima S (1984) Phil Mag A 49:845
7. Maksimova EL, Shvindlerman LS, Straumal BB (1988) Acta Metall 36:1573
8. Divinski S, Lohmann M, Herzig C, Straumal B, Baretzky B, Gust W (2005) Phys Rev B 71: art.no. 104104
9. Hsieh T, Balluffi R (1989) Acta Metall 37:1637
10. Alsayed A, Islam MF, Zhang J, Collings PJ, Yodh AG (2005) Science 309:1207
11. Luo J, Gupta VK, Yoon DH, Meyer HM (2005) App Phys Lett 87: art.no. 231902
12. Kikuchi R, Cahn JW (1980) Phys Rev B 21:1893
13. Kikuchi R, Cahn JW (1987) Phys Rev B 36:418
14. Broughton JQ, Gilmer GH (1986) Phys Rev Lett 56:2692
15. Ciccotti G, Guillope M, Pontikis V (1983) Phys Rev B 27:5576
16. Nguyen T, Ho PS, Kwok T, Nitta C, Yip S (1986) Phys Rev Lett 57:1919
17. Deymier P, Taiwo A, Kalonji GM (1987) Acta Metall 35:2719
18. Phillpot SR, Lutsko JF, Wolf D, Yip S (1989) Phys Rev B 40:2831
19. Lutsko JF, Wolf D, Phillpot SR, Yip S (1989) Phys Rev B 40:2841
20. Nguyen T, Ho PS, Kwok T, Nitta C, Yip S (1992) Phys Rev B 46:6050
21. Keblinski P, Phillpot SR, Wolf D, Gleiter H (1997) Philos Mag Lett 76:143
22. Besold G, Mouritsen OG (1994) Phys Rev B 50:6573
23. Besold G, Mouritsen OG (2000) Comp Mat Sci 18:225
24. Kobayashi R, Warren JA, Carter WC (2000) Physica D 140:141
25. Warren J, Kobayashi R, Lobkovsky A, Carter W (2003) Acta Mater 51:6035
26. Tang M, Carter WC, Cannon RM (2006) Phys Rev B 73:024102
27. Kobayashiand R, Giga Y (1999) J Stat Phys 95:1187
28. Cahn JW (1997) J Chem Phys 66:3667
29. Tang M, Carter WC, Cannon RM (2006) Phys Rev Lett 97:075502